ESTIMATION PROCESS FOR TIRE-ROAD FORCES AND VEHICLE SIDESLIP ANGLE

Guillaume Baffet, Ali Charara

Heudiasyc Laboratory (UMR CNRS 6599), Université de Technologie de Compiègne
Centre de recherche Royallieu, BP20529 - 60205 Compiègne, France

Daniel Lechner

INRETS-MA Laboratory (Department of Accident Mechanism Analysis)
Chemin de la Croix Blanche, 13300 Salon de Provence, France

Keywords: State observers, vehicle dynamic, sideslip angle estimation, tire-force estimation, wheel cornering stiffness estimation, linear adaptive force model.

Abstract: This study focuses on the estimation of car dynamic variables for the improvement of vehicle safety, handling characteristics and comfort. More specifically, a new estimation process is proposed to estimate longitudinal/lateral tire-road forces, sideslip angle and wheel cornering stiffness. This method uses measurements from currently-available standard sensors (yaw rate, longitudinal/lateral accelerations, steering angle and angular wheel velocities). The estimation process is separated into two blocks: the first block contains an observer whose principal role is to calculate tire-road forces without a descriptive force model, while in the second block an observer estimates sideslip angle and cornering stiffness with an adaptive tire-force model. The different observers are based on an Extended Kalman Filter (EKF). The estimation process is applied and compared to real experimental data, notably sideslip angle and wheel force measurements. Experimental results show the accuracy and potential of the estimation process.

1 INTRODUCTION

The last few years have seen the emergence in cars of active security systems to reduce dangerous situations for drivers. Among these active security systems, Anti-lock Braking Systems (ABS) and Electronic Stability Programs (ESP) significantly reduce the number of road accidents. However, these systems may improved if the dynamic potential of a car is well known. For example, information on tire-road friction means a better definition of potential trajectories, and therefore a better management of vehicle controls. Nowadays, certain fundamental data relating to vehicle-dynamics are not measurable in a standard car for both technical and economic reasons. As a consequence, dynamic variables such as tire forces and sideslip angle must be observed or estimated.

Vehicle-dynamic estimation has been widely discussed in the literature, e.g. ((Kiencke and Nielsen, 2000), (Ungoren et al., 2004), (Lechner, 2002), (Stephant et al., 2006)). The vehicle-road system is usually modeled by combining a vehicle model with a tire-force model in one block. One particularity

of this study is to separate the estimation modeling into two blocks (shown in figure 1), where the first block concerns the car body dynamic while the second is devoted to the tire-road interface dynamic. The
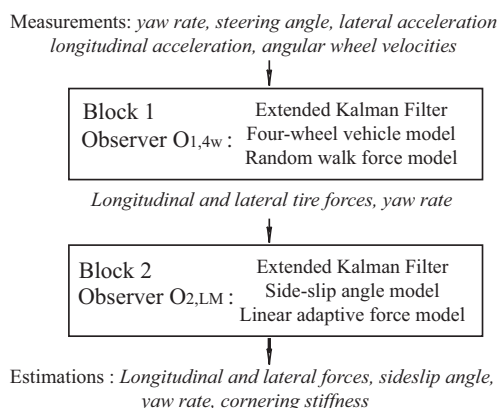
Measurements: *yaw rate, steering angle, lateral acceleration longitudinal acceleration, angular wheel velocities*

Estimations : *Longitudinal and lateral forces, sideslip angle, yaw rate, cornering stiffness*

Figure 1: Estimation process. Observers $O_{1,4w}$ and $O_{2,LAM}$.

first block contains an Extended Kalman Filter (denoted as $O_{1,4w}$) constructed with a four-wheel vehicle

model and a random walk force model. The first observer $O_{1,4w}$ estimates longitudinal/lateral tire forces and yaw rate, which are inputs to the observer in the second block (denoted as $O_{2,LAM}$). This second observer is developed from a sideslip angle model and a linear adaptive force model.

Some studies have described observers which take road friction variations into account ((Lakehal-ayat et al., 2006), (Rabhi et al., 2005), (Ray, 1997)). In the works of (Lakehal-ayat et al., 2006) road friction is considered as a disturbance. Alternatively, as in (Rabhi et al., 2005), the tire-force parameters are identified with an observer, while in (Ray, 1997) tire forces are modeled with an integrated random walk model. In this study a linear adaptive tire force model is proposed (in block 2) with an eye to studying road friction variations.

The rest of the paper is organized as follows. The second section describes the vehicle model and the observer $O_{1,4w}$ (block 1). Next, the third section presents the sideslip angle and cornering stiffness observer ($O_{2,LAM}$ in block 2). In the fourth section an observability analysis is performed. The fifth section provides experimental results: the two observers are evaluated with respect to sideslip angle and tire force measurements. Finally, concluding remarks are given in section 6.

2 BLOCK 1: OBSERVER FOR TIRE-ROAD FORCE

This section describes the first observer $O_{1,4w}$ constructed from a four-wheel vehicle model (figure 2), where $\dot{\psi}$ is the yaw rate, β the center of gravity
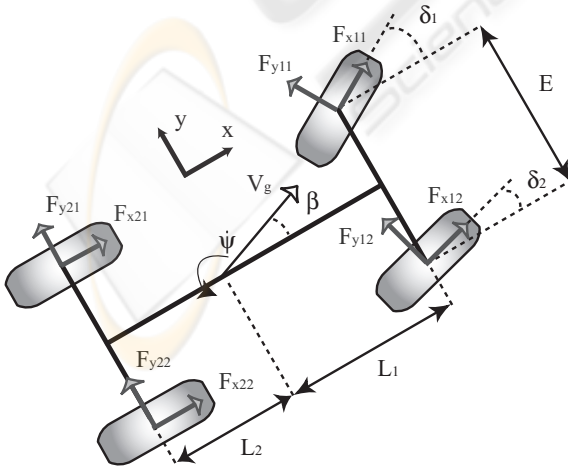
Figure 2: Four-wheel vehicle model.

sideslip angle, V_g the center of gravity velocity, and L_1 and L_2 the distance from the vehicle center of gravity to the front and rear axles respectively. $F_{x,y,i,j}$ are the longitudinal and lateral tire-road forces, $\delta_{1,2}$ are the front left and right steering angles respectively, and E is the vehicle track (lateral distance from wheel to wheel).

In order to develop an observable system (notably in the case of null steering angles), rear longitudinal forces are neglected relative to the front longitudinal forces. The simplified equation for yaw acceleration (four-wheel vehicle model) can be formulated as the following dynamic relationship ($O_{1,4w}$ model):

$$\ddot{\psi} = \frac{1}{I_z} \begin{bmatrix} L_1[F_{y11}\cos(\delta_1) + F_{y12}\cos(\delta_2) \\ +F_{x11}\sin(\delta_1) + F_{x12}\sin(\delta_2)] \\ -L_2[F_{y21} + F_{y22}] \\ +\frac{E}{2}[F_{y11}\sin(\delta_1) - F_{y12}\sin(\delta_2) \\ +F_{x12}\cos(\delta_2) - F_{x11}\cos(\delta_1)] \end{bmatrix}, \quad (1)$$

where m the vehicle mass and I_z the yaw moment of inertia. The different force evolutions are modeled with a random walk model:

$$[\dot{F_{xij}}, \dot{F_{yij}}] = [0,0], \quad i = 1,2 \quad j = 1,2. \quad (2)$$

The measurement vector Y and the measurement model are:

$$\begin{aligned} Y &= [\dot{\psi}, \gamma_y, \gamma_x] = [Y_1, Y_2, Y_3], \\ Y_1 &= \dot{\psi}, \\ Y_2 &= \frac{1}{m}[F_{y11}\cos(\delta_1) + F_{y12}\cos(\delta_2) \\ &\quad +(F_{y21} + F_{y22}) + F_{x11}\sin(\delta_1) + F_{x12}\sin(\delta_2)], \\ Y_3 &= \frac{1}{m}[-F_{y11}\sin(\delta_1) - F_{y12}\sin(\delta_2) \\ &\quad +F_{x11}\cos(\delta_1) + F_{x12}\cos(\delta_2)], \end{aligned} \quad (3)$$

where γ_x and γ_y are the longitudinal and lateral accelerations respectively.

The $O_{1,4w}$ system (association between equations (1), random walk force equation (2), and the measurement equations (3)) is not observable in the case where F_{y21} and F_{y22} are state vector components. For example, in equation (1, 2, 3) there is no relation allowing to distinguish the rear lateral forces F_{y21} and F_{y22} in the sum ($F_{y21}+F_{y22}$): as a consequence only the sum ($F_{y2} = F_{y21} + F_{y22}$) is observable. Moreover, when driving in a straight line, yaw rate is small, δ_1 and δ_2 are approximately null, and hence there is no significant knowledge in equation (1, 2, 3) differentiating F_{y11} and F_{y12} in the sum ($F_{y11} + F_{y12}$), so only the sum ($F_{y1} = F_{y11} + F_{y12}$) is observable. These observations lead us to develop the $O_{1,4w}$ system with a state vector composed of force sums:

$$X = [\dot{\psi}, F_{y1}, F_{y2}, F_{x1}], \quad (4)$$

where F_{x1} is the sum of front longitudinal forces ($F_{x1} = F_{x11} + F_{x12}$). Tire forces and force sums are as-

sociated according to the dispersion of vertical forces:

$$F_{x11} = \frac{F_{z11}F_{x1}}{F_{z12}+F_{z11}}, \quad F_{x12} = \frac{F_{z12}F_{x1}}{F_{z12}+F_{z11}}, \quad (5)$$

$$F_{y11} = \frac{F_{z11}F_{y1}}{F_{z12}+F_{z11}}, \quad F_{y12} = \frac{F_{z12}F_{y1}}{F_{z12}+F_{z11}}, \quad (6)$$

$$F_{y21} = \frac{F_{z21}F_{y2}}{F_{z22}+F_{z21}}, \quad F_{y22} = \frac{F_{z22}F_{y2}}{F_{z22}+F_{z21}}, \quad (7)$$

where F_{zij} are the vertical forces. These are calculated, neglecting roll and suspension movements, with the following load transfer model:

$$F_{z11} = \frac{L_2mg - h_{cog}m\gamma_x}{2(L_1+L_2)} - \frac{L_2h_{cog}m\gamma_y}{(L_1+L_2)E}, \quad (8)$$

$$F_{z12} = \frac{L_2mg - h_{cog}m\gamma_x}{2(L_1+L_2)} + \frac{L_2h_{cog}m\gamma_y}{(L_1+L_2)E}, \quad (9)$$

$$F_{z21} = \frac{L_1mg + h_{cog}m\gamma_x}{2(L_1+L_2)} - \frac{L_2h_{cog}m\gamma_y}{(L_1+L_2)E}, \quad (10)$$

$$F_{z22} = \frac{L_1mg + h_{cog}m\gamma_x}{2(L_1+L_2)} + \frac{L_2h_{cog}m\gamma_y}{(L_1+L_2)E}, \quad (11)$$

h_{cog} being the center of gravity height and g the gravitational constant. The load transfer model follows the assumption of the superposition principle of independent longitudinal and lateral acceleration contributions (Lechner, 2002). The input vectors U of $O_{1,4w}$ observer is:

$$U = [\delta_1, \delta_2, F_{z11}, F_{z12}, F_{z21}, F_{z22}]. \quad (12)$$

As regards the vertical force inputs, these are calculated from lateral and longitudinal accelerations with the load transfer model.

3 BLOCK 2: OBSERVER FOR SIDESLIP ANGLE AND CORNERING STIFFNESS

This section presents the observer $O_{2,LAM}$ constructed from a sideslip angle model and a tire-force model. The sideslip angle model is based on the single-track model (Segel, 1956), with neglected rear longitudinal force:

$$\dot{\beta} = \frac{F_{x1}\sin(\delta-\beta) + F_{y1}\cos(\delta-\beta) + F_{y2}\cos(\beta)}{mV_g} - \dot{\psi}. \quad (13)$$

Rear and front sideslip angles are calculated as:

$$\begin{aligned} \beta_1 &= \delta - \beta - L_1\dot{\psi}/V_g, \\ \beta_2 &= -\beta + L_2\dot{\psi}/V_g, \end{aligned} \quad (14)$$

where δ is the mean of front steering angles.

The dynamic of the tire-road contact is usually formulated by modeling the tire-force as a function of

the slip between tire and road ((Pacejka and Bakker, 1991), (Kiencke and Nielsen, 2000), (Canudas-De-Wit et al., 2003)). Figure 3 illustrates different lateral tire-force models (linear, linear adaptive and Burckhardt for various road surfaces (Kiencke and Nielsen, 2000)). In this study lateral wheel slips are assumed to be equal to the wheel sideslip angles. In current driv-
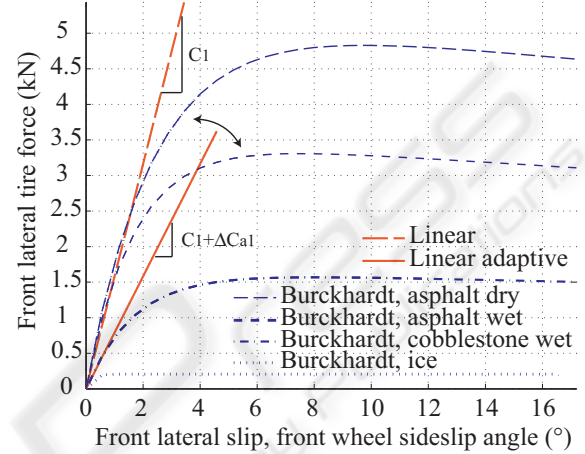

Figure 3: Lateral tire force models: linear, linear adaptive, Burckhardt for various road surfaces.

ing situations, lateral tire forces may be considered linear with respect to sideslip angle (linear model):

$$F_{yi}(\beta_i) = C_i\beta_i, \qquad i = 1, 2, \quad (15)$$

where C_i is the wheel cornering stiffness, a parameter closely related to tire-road friction.

When road friction changes or when the nonlinear tire domain is reached, "real" wheel cornering stiffness varies. In order a take the wheel cornering stiffness variations into account, we proposed an adaptive tire-force model (named the linear adaptive tire-force model, illustrated in figure 3). This model is based on the linear model at which a readjustment variable ΔC_{ai} is added to correct wheel cornering stiffness errors:

$$F_{yi}(\beta_i) = (C_i + \Delta C_{ai})\beta_i. \quad (16)$$

The variable ΔC_{ai} is included in the state vector of the $O_{2,LAM}$ observer and it evolution equation is formulated according to a random walk model ($\dot{\Delta C_{ai}} = 0$). State $X' \in R^3$, input $U' \in R^4$ and measurement $Y' \in R^3$ are chosen as:

$$\begin{aligned} X' &= [x'_1, x'_2, x'_3] = [\beta, \Delta C_{a1}, \Delta C_{a2}], \\ U' &= [u'_1, u'_2, u'_3, u'_4] = [\delta, \dot{\psi}, V_g, F_{x1}], \\ Y' &= [y'_1, y'_2, y'_3] = [F_{y1}, F_{y2}, \gamma_y]. \end{aligned} \quad (17)$$

The measurement model is

$$
\begin{aligned}
y'_1 &= (C_1 + x'_2)\beta_1, \\
y'_2 &= (C_2 + x'_3)\beta_2, \\
y'_3 &= \frac{1}{m}[(C_1 + x'_2)\beta_1 \cos(u'_1) + (C_2 + x'_3)\beta_2 \\
&\quad + u'_4 \sin(u'_1)].
\end{aligned}
\tag{18}
$$

where

$$
\begin{aligned}
\beta_1 &= u'_1 - x'_1 - L_1 u'_2/u'_3, \\
\beta_2 &= -x'_1 + L_2 u'_2/u'_3.
\end{aligned}
\tag{19}
$$

Consider the state estimation denoted as $\widehat{X}' = [\widehat{x_1}', \widehat{x_2}', \widehat{x_3}']$, the state evolution model of $O_{2,LAM}$ is:

$$
\begin{aligned}
\dot{\widehat{x_1}}' &= \frac{1}{mu_3}[u'_4 \sin(u'_1 - \widehat{x_1}') + F_{yw1,aux} \cos(u'_1 - \widehat{x_1}') \\
&\quad + F_{yw2,aux} \cos(\widehat{x_1}')] - u'_2, \\
\dot{\widehat{x_2}}' &= 0, \\
\dot{\widehat{x_3}}' &= 0,
\end{aligned}
\tag{20}
$$

where the auxiliary variables $F_{yw1,aux}$ and $F_{yw2,aux}$ are calculated as:

$$
\begin{aligned}
F_{yw1,aux} &= (C_1 + \widehat{x_2}')(u'_1 - \widehat{x_1}' - L_1 u'_2/u'_3), \\
F_{yw2,aux} &= (C_2 + \widehat{x_3}')(-\widehat{x_1}' + L_2 u'_2/u'_3).
\end{aligned}
\tag{21}
$$

4 OBSERVABILITY

The different observers ($O_{1,4w}$, $O_{2,LAM}$) were developed according to an extended Kalman filter method (Kalman, 1960), (Mohinder and Angus, 1993).

The two observer systems are nonlinear, so the two observability functions were calculated using a lie derivative method (Nijmeijer and der Schaft, 1990). Ranks of the two observability functions corresponded to the state vector dimensions, so systems $O_{1,4w}$ and $O_{2,LAM}$ were locally observable. Concerning the observability of the complete systems ($O_{1,4w}$ and $O_{2,LAM}$), a previous work (Baffet et al., 2006a) showed that a similar system (in one block) is locally observable.

5 EXPERIMENTAL RESULTS

The experimental vehicle (see figure 4) is a Peugeot 307 equipped with a number of sensors including GPS, accelerometer, odometer, gyrometer, steering angle, correvit and dynamometric hubs. Among these sensors, the correvit (a non-contact optical sensor) gives measurements of rear sideslip angle and vehicle velocity, while the dynamometric hubs are wheel-force transducers.

This study uses an experimental test representative of both longitudinal and lateral dynamic behaviors.
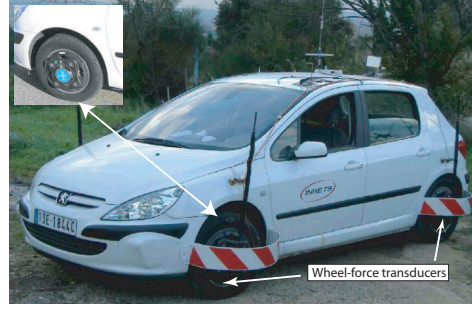

Figure 4: Laboratory's experimental vehicle.

The vehicle trajectory and the acceleration diagram are shown in figure 5. During the test, the vehicle first accelerated up to $\gamma_x \approx 0.3g$, then negotiated a slalom at an approximate velocity of $12m/s$ ($-0.6g < \gamma_y < 0.6g$), before finally decelerating to $\gamma_x \approx -0.7g$. The
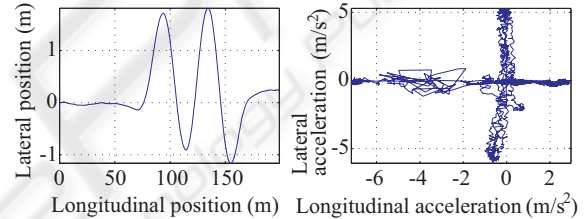

Figure 5: Experimental test, vehicle positions, acceleration diagram.

results are presented in two forms: figures of estimations/measurements and tables of normalized errors. The normalized error ε_z for an estimation z is defined in (Stephant et al., 2006) as

$$
\varepsilon_z = 100(\|z - z_{measurement}\|)/(\max \|z_{measurement}\|).
\tag{22}
$$

5.1 Block 1: Observer $O_{1,4w}$ Results

Figure 6 and table 1 present $O_{1,4w}$ observer results. The state estimations were initialized using the maximum value of the measurements during the test (for instance, the estimation of the front lateral force F_{y1}

Table 1: Maximum absolute values, $O_{1,4w}$ normalized mean errors and normalized standard deviation (Std).

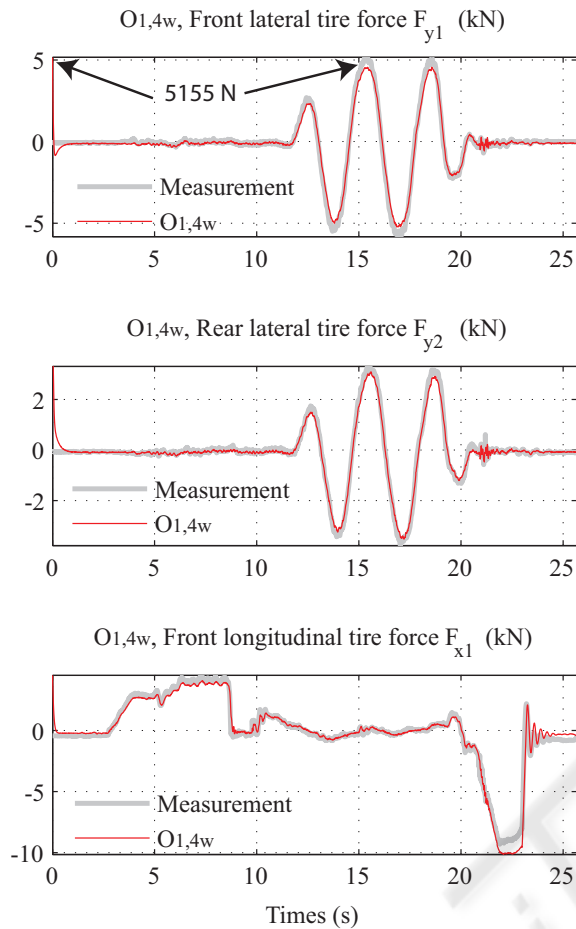|	max $\|\|\|$	Mean	Std
F_{y1}	5816 N	3.1%	4.0%
F_{y2}	3782 N	2.9%	5.4%
F_{x1}	9305 N	3.1%	4.1%
$\dot\psi$	24.6 $^o/s$	0.4%	2.6%

Figure 6: Experimental test. $O_{1,4w}$ results in comparison with measurements.

was set to 5155 N). In spite of these false initializations the estimations converge quickly to the measured values, showing the good convergence properties of the observer. Moreover, the $O_{1,4w}$ observer produces satisfactory estimations close to measurements (normalized mean and standard deviations errors are less than 7 %). These good experimental results confirm that the observer approach may be an appropriate way for the estimation of tire-forces.

5.2 Block 2: Observer $O_{2,LAM}$ Results

During the test, (F_{x1}, F_{y1}, F_{y2}) inputs of $O_{2,LAM}$ were originally those from the $O_{1,4w}$ observer. The V_g input of $O_{2,LAM}$ was obtained from the wheel angular velocities. In order to demonstrate the improvement provided by the observer using the *linear adaptive force model* ($O_{2,LAM}$, equation 16), another observer constructed with a *linear fixed force model* is used

in comparison (denoted O_{rl}, equation 15, described in (Baffet et al., 2006b)). The robustness of the two observers is tested with respect to tire-road friction variations by performing the tests with different cornering stiffness parameters ($[C_1, C_2] * 0.5, 1, 1.5$). The observers were evaluated for the same test presented in section 5.

Figure 7 shows the estimation results of observer O_{rl} for rear sideslip angle. Observer O_{rl} gives good results when cornering stiffnesses are approximately known ($[C_1, C_2] * 1$). However, this observer is not robust when cornering stiffnesses change ($[C_1, C_2] * 0.5, 1.5$).
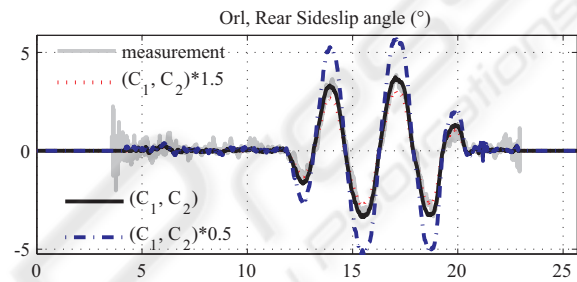

Figure 7: Observer O_{rl} using a fixed linear force model, rear sideslip angle estimations with different cornering stiffness settings.

Figure 8 and table 2 show estimation results for the adaptive observer $O_{2,LAM}$. The performance robustness of $O_{2,LAM}$ is very good, since sideslip angle is well estimated irrespective of cornering stiffness settings. This result is confirmed by the normalized mean errors (Table 2) which are approximately constant (about 7 %). The front and rear cornering stiffness estimations ($C_i + \Delta C_i$) converge quickly to the same values after the beginning of the slalom at 12 s.

Table 2: Observer O_{LAM}, rear sideslip angle estimation results, maximum absolute value, normalized mean errors.

$O_{2,LAM}$	$0.5(C_1, C_2)$	(C_1, C_2)	$1.5(C_1, C_2)$
max $\|\beta_2\|$	3.0^o	3.0^o	3.0^o
Mean	7.4%	7.0%	7.2%

6 CONCLUSIONS AND FUTURE WORK

This study deals with two vehicle-dynamic observers constructed for use in a two-block estimation process. Experimental results show that the first observer $O_{1,4w}$ gives force estimations close to the measurements, and the second observer $O_{2,LAM}$ provides good
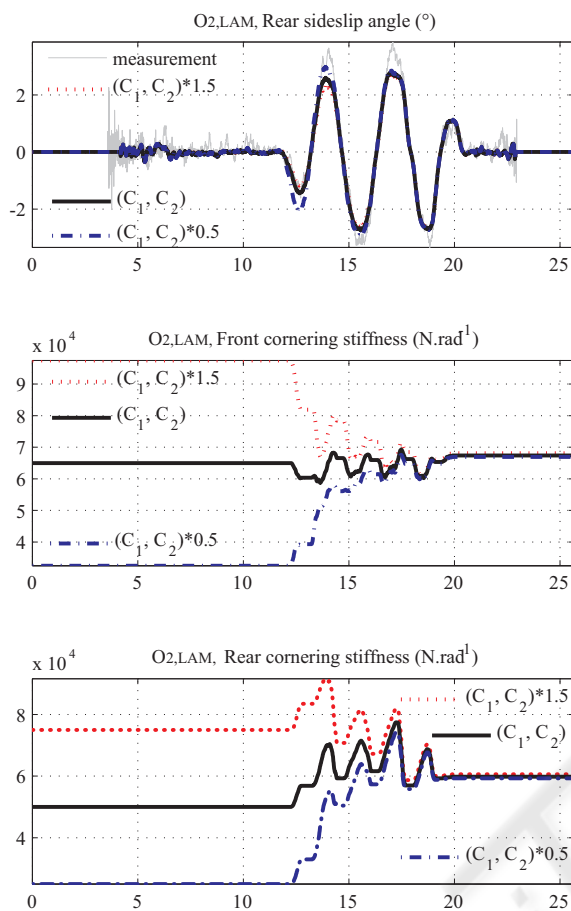
Figure 8: $O_{2,LAM}$ adaptive observer, Sideslip angle estimation results, Front and rear cornering stiffness estimations $C_i + \Delta C_i$, with different cornering stiffness settings.

sideslip angle estimations with good robustness properties relative to cornering stiffness changes. This result justifies the use of an adaptive tire-force model to take into account road friction changes.

Future studies will improve vehicle/road models in order to widen validity domains for observers. Subsequent vehicle/road models will take into account roll and vertical dynamics.

REFERENCES

Baffet, G., Stephant, J., and Charara, A. (2006a). Sideslip angle lateral tire force and road friction estimation in simulations and experiments. Proceedings of the IEEE conference on control application CCA Munich Germany.

Baffet, G., Stephant, J., and Charara, A. (2006b). Vehicle sideslip angle and lateral tire-force estimations in

standard and critical driving situations: Simulations and experiments. Proceedings of the 8th International Symposium on Advanced Vehicle Control AVEC2006 Taipei Taiwan.

Canudas-De-Wit, C., Tsiotras, P., Velenis, E., Basset, M., and Gissinger, G. (2003). Dynamic friction models for road/tire longitudinal interaction. volume 39, pages 189–226. Vehicle System Dynamics.

Kalman, R. E. (1960). A new approach to linear filtering and prediction problems. volume 82, pages 35–45. Transactions of the ASME - PUBLISHER of Basic Engineering.

Kiencke, U. and Nielsen, L. (2000). Automotive control system. Springer.

Lakehal-ayat, M., Tseng, H. E., Mao, Y., and j. Karidas (2006). Disturbance observer for lateral velocity estimation. Proceedings of the 8th International Symposium on Advanced Vehicle Control AVEC2006 Taipei Taiwan.

Lechner, D. (2002). Analyse du comportement dynamique des vehicules routiers legers: developpement d'une methodologie appliquee a la securite primaire. Ph.D. dissertation Ecole Centrale de Lyon France.

Mohinder, S. G. and Angus, P. A. (1993). Kalman filtering theory and practice. Prentice hall.

Nijmeijer, H. and der Schaft, A. J. V. (1990). Nonlinear dynamical control systems. Springer-Verlag.

Pacejka, H. B. and Bakker, E. (1991). The magic formula tyre model. pages 1–18. Int. colloq. on tyre models for vehicle dynamics analysis.

Rabhi, A., M'Sirdi, N. K., Zbiri, N., and Delanne, Y. (2005). Vehicle-road interaction modelling for estimation of contact forces. volume 43, pages 403–411. Vehicle System Dynamics.

Ray, L. (1997). Nonlinear tire force estimation and road friction identification : Simulation and experiments. volume 33, pages 1819–1833. Automatica.

Segel, M. L. (1956). Theorical prediction and experimental substantiation of the response of the automobile to steering control. volume 7, pages 310–330. automobile division of the institut of mechanical engineers.

Stephant, J., Charara, A., and Meizel, D. (Available online 5 June 2006). Evaluation of a sliding mode observer for vehicle sideslip angle. Control Engineering Practice.

Ungoren, A. Y., Peng, H., and Tseng, H. E. (2004). A study on lateral speed estimation methods. volume 2, pages 126–144. Int. J. Vehicle Autonomous Systems.